International Journal of Bifurcation and Chaos, Vol. 19, No. 4 (2009) 1357–1366
© World Scientific Publishing Company

DYNAMICS OF A SIMPLIFIED LORENZ SYSTEM

KEHUI SUN
School of Physics Science and Technology, Central South University, Changsha 410083, P. R. China
kehui@csu.edu.cn

J. C. SPROTT
Department of Physics, University of Wisconsin, Madison, WI 53706, USA
sprott@physics.wisc.edu

Received June 4, 2008; Revised September 12, 2008

A simplified Lorenz system with one bifurcation parameter is investigated by a detailed theoretical analysis as well as dynamic simulation, including some basic dynamical properties, Lyapunov exponent spectra, fractal dimension, bifurcations and routes to chaos. The results show that this system has complex dynamics with interesting characteristics.

Keywords: Chaos; Lorenz system; Lyapunov exponent; bifurcation.

1. Introduction

In 1963, Lorenz launched the modern era of chaos when he reported sensitive dependence on initial condition in a three-dimensional autonomous system of ordinary differential equations as a simple model of atmospheric convection [Lorenz, 1963; Stewart, 2000]. Subsequently, his system has been extensively studied with many important results in chaotic dynamics, control and synchronization. Although there are only three adjustable parameters in his system, they comprise a huge parameter space that has only been partially explored. In 1999, Chen constructed a 3-D chaotic system by a simple state feedback to the second equation in the Lorenz system [Chen & Ueta, 1999] that combines features of both the Lorenz attractor and the Rössler attractor [Rössler, 1976]. Shortly thereafter, Lü and Chen [2002] investigated another similar system by removing the x term and changing the sign of the y term in the $\dot{y}$ equation of the Lorenz system. Despite its similar structure to the Lorenz system, they are not topologically equivalent [Ueta & Chen, 2000]. In a sense defined by Vaněček and Čelikovský [1996], the Lorenz system satisfies the condition $a_{12}a_{21} > 0$, while the Chen system satisfies $a_{12}a_{21} < 0$, and the Lü system satisfies the condition $a_{12}a_{21} = 0$. Soon thereafter, a so-called Lorenz system family was constructed [Lü *et al.*, 2002] as a connection of the Lorenz, Lü and Chen systems by the variation of a single real parameter. In 2001, using only passive nonlinear devices, Elwakil constructed a modified Lorenz system which is represented by three equations with no multipliers, but it is asymmetrical, and its parameters are constant [Elwakil & Kennedy, 2001]. Recently, Qi reported a new system by adding a cross-product nonlinear term to the first equation of the Lorenz system [Qi *et al.*, 2005]. This system has three parameters and exhibits complex dynamics and structure.

We report here two simplifications of the Lorenz system in which the x and y terms in the $\dot{y}$ equation are separately set to zero while retaining the chaos with a linear trajectory through parameter space that connects these two simple cases with the classic

Lorenz system. It has the same features as the system studied by Lü *et al.* [2002], but a simpler algebraic form. In particular, the adjustable parameter occurs in only two of the terms rather than in four. The plan of the paper is as follows. In Sec. 2, we present the simplified Lorenz system and its basic properties. In Sec. 3, we describe the dynamics and bifurcations of the system. Finally, we summarize the results and indicate future directions.

2. The Simplified Lorenz System and its Basic Properties

We consider the Lorenz system with a single adjustable parameter c described by

$$\begin{cases} \dot{x} = 10(y - x) \\ \dot{y} = -xz + (24 - 4c)x + cy \\ \dot{z} = xy - \dfrac{8z}{3} \end{cases} . \tag{1}$$

Here, c is the bifurcation parameter. The attractor is shown in Fig. 1 for $c = 2$.

The system (1) has the following features:

(i) It is chaotic over most of the range $c \in [-1.59, 7.75]$.
(ii) For $c = -1$, it is the usual Lorenz system with the standard parameters.
(iii) For $c = 0$, the variable y is removed from the second equation.
(iv) For $c = 6$, the variable x is removed from the second equation.
(v) There is a rich set of bifurcations as c is varied over the range.
(vi) According to the topological definition by Vaněček and Čelikovský [1996], the linearization of system (1) about the origin produces a 3×3 constant matrix of partial derivatives, $A = [a_{ij}]_{3\times3}$, in which the sign of $a_{12}a_{21}$ distinguishes nonequivalent topologies. According to this criterion, $a_{12}a_{21} > 0$ when $c < 6$, $a_{12}a_{21} = 0$ when $c = 6$, and $a_{12}a_{21} < 0$ when $c > 6$. Although system (1) includes three different topologies, no special bifurcations were observed at the critical value of $c = 6$. We think the connection between topological structure and dynamics needs further study.

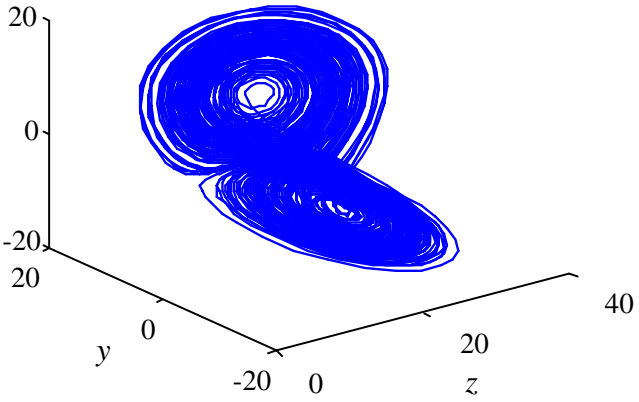

Fig. 1. The chaotic attractor of system (1) for $c = 2$.

Several additional important properties of system (1) will be presented in the following sections.

2.1. *Symmetry and invariance*

System (1) is symmetric and invariant under the transformation $(x, y, z) \to (-x, -y, z)$, i.e. reflection about the z-axis. This symmetry persists for all values of the parameter $c \in (-\infty, \infty)$. Also, the z-axis itself is an orbit (an invariant manifold), i.e. if $x = y = 0$ at $t = t_0$ then $x = y = 0$ for all $t \geq t_0$. Furthermore, the trajectory on the z-axis tends to the origin as $t \to \infty$, since for such a trajectory, $\dot{x} = \dot{y} = 0$ and $\dot{z} = -8z/3$. Therefore, system (1) has this symmetry and invariance for all values of the parameter c.

2.2. *Dissipation and the existence of attractor*

The rate of volume contraction is given by the Lie derivative

$$\frac{1}{V}\frac{dV}{dt} = \sum_i \frac{\partial \dot{\phi}_i}{\partial \phi_i}, \quad i = 1, 2, 3,$$

$$\phi_1 = x, \ \ \phi_2 = y, \ \ \phi_3 = z. \tag{2}$$

For dynamical system (1), we obtain

$$\frac{1}{V}\frac{dV}{dt} = \frac{\partial \dot{x}}{\partial x} + \frac{\partial \dot{y}}{\partial y} + \frac{\partial \dot{z}}{\partial z} = \frac{3c - 38}{3} = p, \tag{3}$$

which can be solved to yield

$$V(t) = V(0)e^{pt}. \tag{4}$$

For $c < 38/3$, p is negative, and the dynamical system (1) is dissipative with solutions for $t \to \infty$ that contract at an exponential rate p onto an attractor of zero volume that may be an equilibrium point, a limit cycle, or a strange attractor.

2.3. *Equilibria and stability*

The equilibria of system (1) can be found by solving the three equations $\dot{x} = \dot{y} = \dot{z} = 0$, which lead to $10(y - x) = 0$, $-xz + (24 - 4c)x + cy = 0$, and $xy - 8z/3 = 0$. There are three equilibria: $S_0(0, 0, 0)$, $S_-(-\sqrt{64 - 8c}, -\sqrt{64 - 8c}, 24 - 3c)$, $S_+(+\sqrt{64 - 8c}, +\sqrt{64 - 8c}, 24 - 3c)$, in which two equilibria, S_- and S_+, are symmetrically placed with respect to the z-axis.

Linearizing system (1) about the equilibrium S_0 provides an eigenvalue $\lambda_1 = -8/3$ along with the following characteristic equation for the other two eigenvalues:

$$f(\lambda) = \lambda^2 + (10 - c)\lambda + 30c - 240 = 0. \tag{5}$$

If $c \in (8, 10)$, then $10 - c > 0$ and $30c - 240 > 0$, thus both eigenvalues of Eq. (5) are negative, i.e. the origin equilibrium is a spiral node. For $c \in (-\infty, 8)$ or $c \in (10, \infty)$, the solution of Eq. (5) always satisfies $\lambda_2 > 0 > \lambda_3$. Therefore, the equilibrium S_0 is a saddle point in the three-dimensional state space.

Next, linearizing the system about the other equilibrium yields the following characteristic equation:

$$f(\lambda) = \lambda^3 + \left(\frac{38}{3} - c\right)\lambda^2 + \left(\frac{272}{3} - \frac{32c}{3}\right)\lambda + 20(64 - 8c). \tag{6}$$

These two equilibria $S_\pm$ have the same stability characterization. Let $A = 38/3 - c$, $B = 272/3 - 32c/3$, $C = 20(64 - 8c)$. For $c \in (-1.59, 7.75)$ or $c \in (8, \infty)$, we have $A > 0$, $B > 0$, $C > 0$ and $A \times B < C$. Thus Eq. (6) does not satisfy the Routh–Hurwitz rule, and there exist a pair of complex conjugate eigenvalues with a positive real part. The two equilibria $S_\pm$ are spiral saddles. If $c \in (-\infty, -1.59)$ or $c \in (7.75, 8)$, then $A \times B > C$. Therefore, Eq. (6) satisfies the Routh–Hurwitz rule, and thus the real part of both complex roots is negative, and so the two equilibria $S_\pm$ are spiral nodes. The classification of equilibria is shown in Table 1.

3. Dynamical Behavior of the System

3.1. *The Lyapunov exponent spectrum*

As it is well known, the Lyapunov exponents measure the exponential rates of divergence and convergence of nearby trajectories in state space, and the Lyapunov exponent spectrum provides additional useful information about the system. The two largest Lyapunov exponents of them are shown in Fig. 2 [Wolf *et al.*, 1985]. A positive and zero Lyapunov exponent indicates chaos, two zero Lyapunov exponents indicate a bifurcation, and a zero and a negative Lyapunov exponent indicates periodicity (a limit cycle).

Note that system (1) is chaotic over most of the range $c \in (-1.59, 7.75)$ with some windows of periodicity in the range $c \in (3.5, 7.75)$, such as $W_1 = [3.507, 3.509]$, $W_2 = [4.581, 4.612]$, $W_3 = [4.6911, 4.722]$, $W_4 = [5.122, 5.127]$, $W_5 = [5.167, 5.169]$, $W_6 = [5.599, 5.600]$, $W_7 = [5.7601, 5.770]$, $W_8 = [5.820, 5.830]$, and $W_9 = [6.415, 6.425]$. Different windows exhibit different periodic obits. Some of these periodic orbits projected onto the xz-plane with different values of c are shown in Fig. 3. For application to secure communication, one should avoid these windows.

3.2. *The Kaplan–Yorke dimension*

Whereas the Lyapunov exponent measures the average predictability of a dynamical system, the dimension of its attractor measures its complexity. A fractional dimension can be defined as in [Kaplan & Yorke, 2003]

$$D_{KY} = D + \frac{1}{|\lambda_{D+1}|}\sum_{j=1}^{D}\lambda_j. \tag{7}$$

The Kaplan–Yorke dimension of system (1) is shown in Fig. 4. The dimension of system (1) is larger than 2 for a strange attractor, and is 1.0 for a limit cycle, and zero for a stable equilibrium. The system has no stable equilibria over the range $c \in (-1.59, 7.75)$.

Table 1. Classification of equilibrium points for different values of c.

Equilibria	c	Sign of eigenvalues	Classification
S_0	$(8, 10)$	$---$	spiral node
	$(-\infty, 8)$ & $(10, \infty)$	$+--$	saddle point (Index 1)
$S_\pm$	$(-\infty, -1.59)$ & $(7.75, 8)$	$---$	spiral node
	$(-1.59, 7.75)$	$++-$	spiral saddle (Index 2)
	$(8, \infty)$	$+--$	saddle point (Index 1)

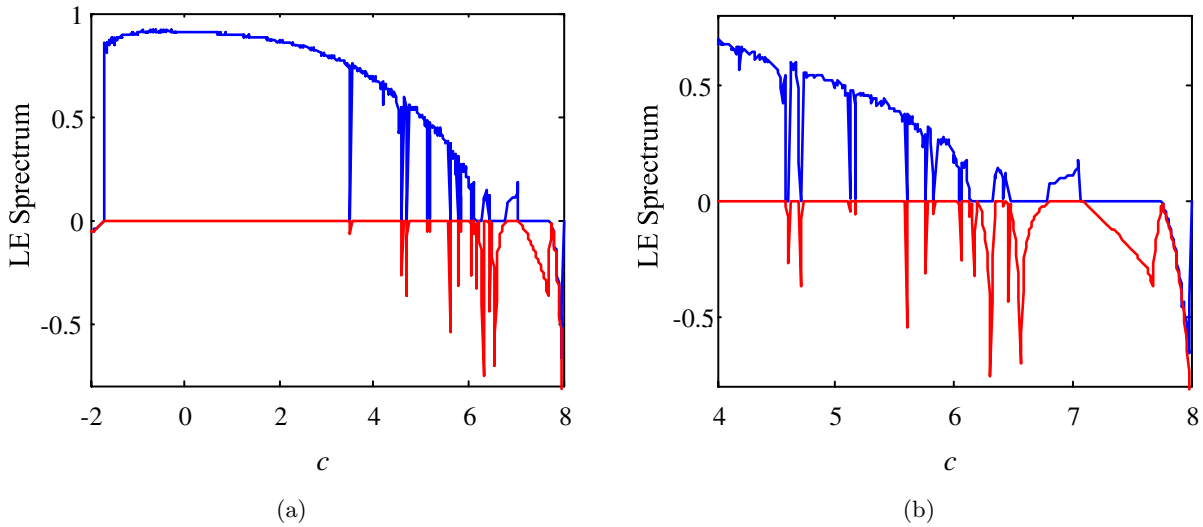

Fig. 2. The two largest Lyapunov exponents (blue and red, respectively) versus c: (a) $c \in (-2, 8)$, (b) $c \in (4, 8)$ (Time step: 0.01, Initial condition: (0, −0.01, 9), Iterations: 800 000).

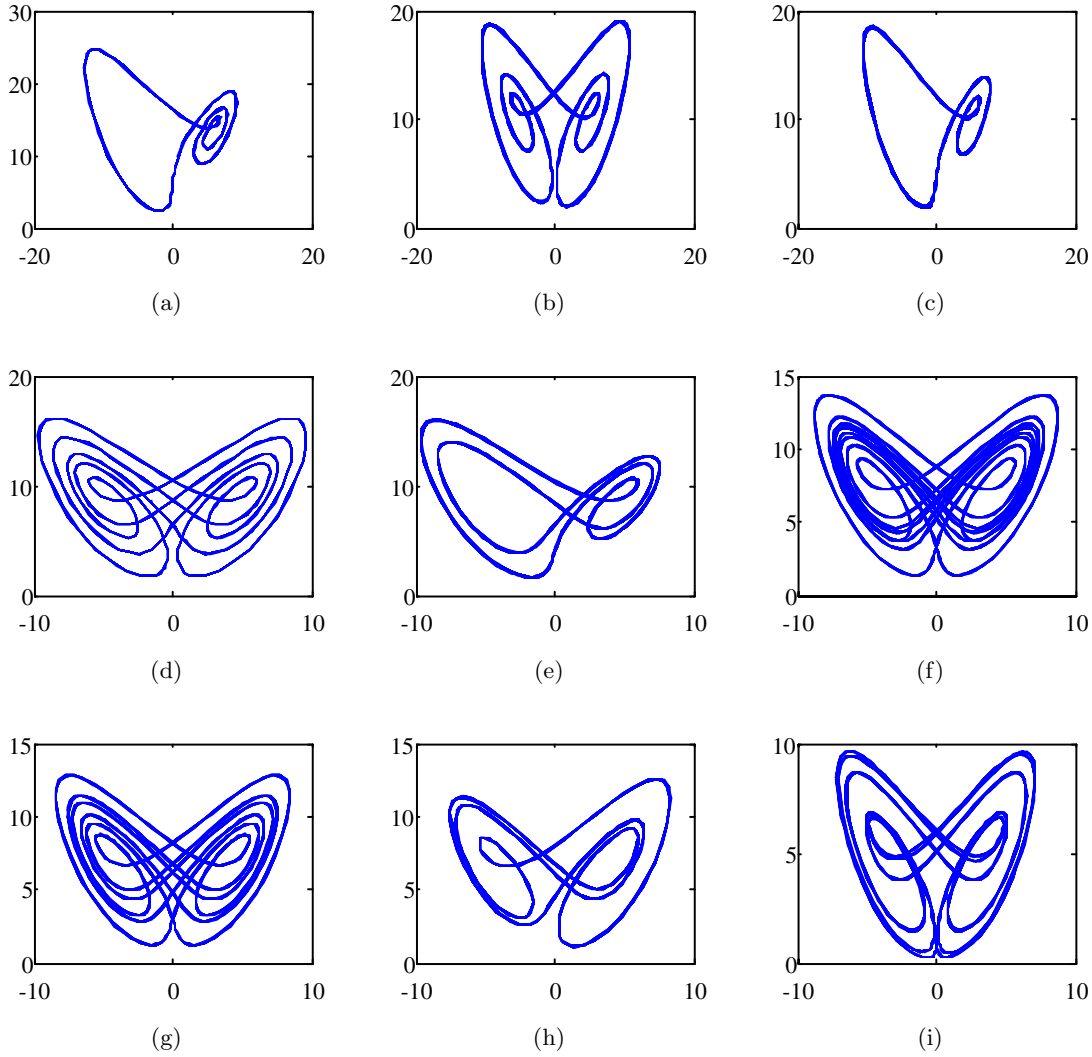

Fig. 3. Periodic orbits of system (1) projected onto the xz-plane for different values of c: (a) $c = 3.509$, (b) $c = 4.590$, (c) $c = 4.701$, (d) $c = 5.124$, (e) $c = 5.169$, (f) $c = 5.600$, (g) $c = 5.770$, (h) $c = 5.828$, (i) $c = 6.42$.

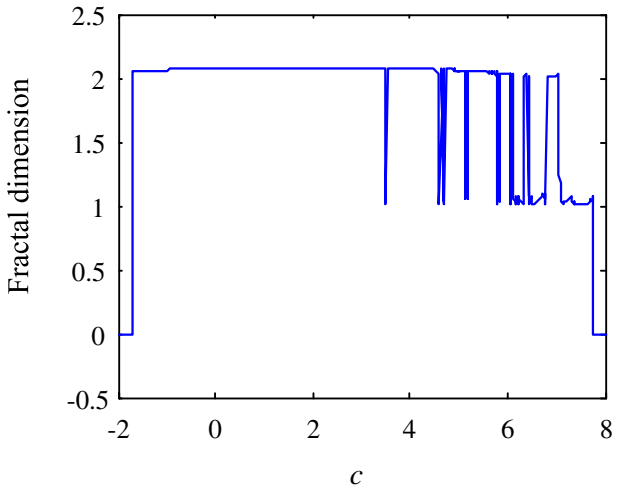

Fig. 4. The Kaplan–Yorke dimension of system (1).

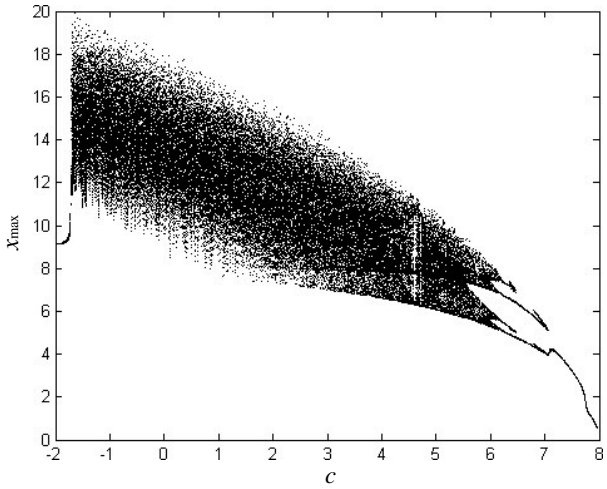

Fig. 5. The bifurcation diagram of $x_{\max}$ versus c.

3.3. *Routes to chaos*

The range of dynamical behaviors is shown by the bifurcation diagram in Fig. 5 in which successive values of $x_{\max}$ are plotted at each value of c. The band structure indicates chaos, which disappears as c increases. On the other hand, the transition from chaos is apparently different at the two extremes of c. All of the dynamics are summarized in Table 2, and the detailed analysis will be presented in following sections.

3.3.1. *From transient chaos, boundary crisis, hysteresis and Hopf bifurcation to chaos*

When c increases from $-\infty$ to -1.6499, there exist two stable equilibria and an unstable equilibrium in system (1). The trajectory wanders in the vicinity of the saddle point at the origin, exhibiting transient chaos. For example, the solution of (1) for $c = -1.8$ exhibits a transient chaotic behavior as shown in Fig. 6(a) which suddenly switches to a

Table 2. Route to chaos in Eq. (1).

c	LE	Dimension	Dynamics
$(-\infty, -1.6499)$	$-\ -\ -$	0	Transient chaos
-1.6499	$+\ 0\ -$	> 2	Boundary crisis
$(-1.6499, -1.5903)$	$+\ 0\ -$	1, >2	Multiple coexisting attractors, hysteresis
-1.5903	$0\ \ 0\ -$		Subcritical Hopf bifurcation
$(-1.5903, 6.44)$	$+\ 0\ -$	> 2	Chaos (with periodic windows)
(6.45, 6.79)	$0\ -\ -$	1	Limit cycles
6.60	$0\ \ 0\ -$	1	Pitchfork bifurcation
(6.60, 6.46)	$0\ \ 0\ -$	1	Limit cycles
6.46	$0\ \ 0\ -$	1	Period-doubling bifurcation
(6.46, 6.80)	$0\ \ 0\ -$	1	Limit cycles
(6.80, 7.054)	$+\ 0\ -$	> 2	Chaos
7.054	$0\ -\ -$		Homoclinic bifurcation
(7.054, 7.6792)	$0\ \ 0\ -$	1	Limit cycles
7.6792	$0\ -\ -$	1	Two Limit circles merging
(7.6792, 7.7567)	$0\ \ 0\ -$	1	Limit cycles
7.7567	$0\ \ 0\ -$		Supercritical Hopf bifurcation
(7.7567, 8)	$-\ -\ -$	0	Two stable equilibria
8	$0\ -\ -$	0	Pitchfork bifurcation
(8, 10)	$-\ -\ -$	0	One stable equilibrium
10	$0\ \ 0\ -$		Subcritical Hopf bifurcation
$(10, \infty)$			Unbounded orbits

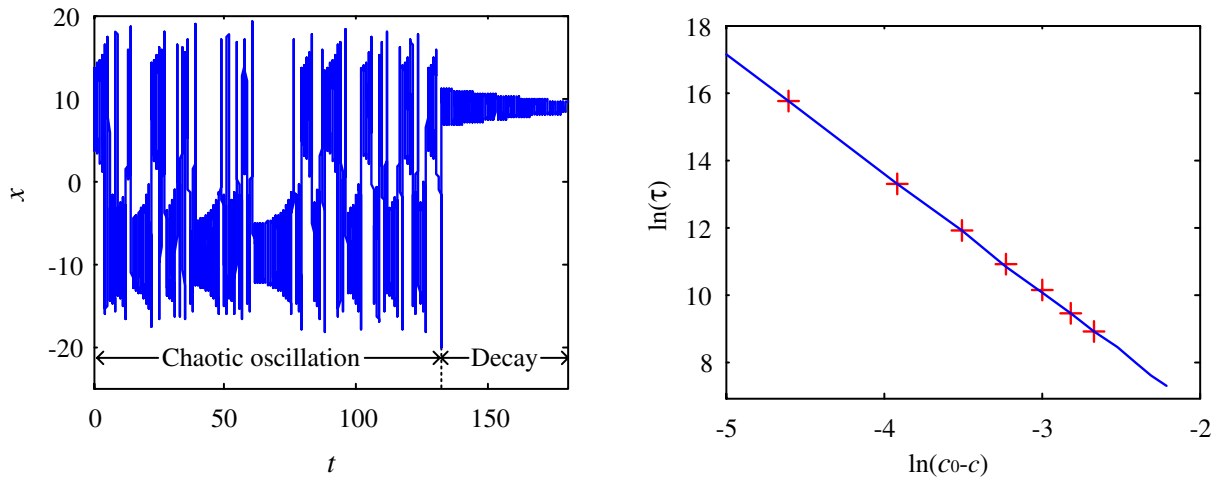

Fig. 6. Transient chaotic behavior in system (1). (a) Transient chaos for $c = -1.80$, IC: (10.0846, 4.6516, 36.5640); (b) Duration of transient chaos in system (1).

pattern of oscillation that decays to the equilibrium $x = \sqrt{64 - 8c}$. On the average, chaotic behavior switches to damped behavior after about 130 oscillations. For larger $c < c_0 \approx -1.6499$, chaotic behavior persists longer. Similar behavior has been reported for the standard Lorenz system [Yorke & Yorke, 1979]. By a numerical experiment with 400 point average for each value of c, we find the scaling for the duration of the chaotic transient (τ) as a function of c as shown in Fig. 6(b). Nonlinear regression of the seven data points leads to the result

$$\ln(\tau) = -3.5131 \ln(c_0 - c) - a, \qquad (8)$$

where $c_0 = -1.6499$, $a = 0.4084$. The transient chaos is especially long-lived (superpersistent) when c is close to c_0, and has been observed in coupled chaotic electrical oscillators [Zhu *et al.*, 2001].

At $c = -1.6499$, the system undergoes a boundary crisis when the strange attractor collides with the basin of attraction separating it from the two attracting equilibrium points. After the crisis, the strange attractor coexists with the two stable equilibria for $c \in (-1.6499, -1.5903)$, and the system exhibits hysteresis, in which the bifurcation occurs at different values of the parameter depending on the direction in which it is changed.

At $c = -1.5903$, the stable equilibria $S_\pm$ become unstable spiral saddles with index 2 (the index is the dimension of the unstable manifold). The eigenvalues, which are a complex conjugate pair, cross the imaginary axis, and the oscillation changes from decay to growth in a subcritical Hopf bifurcation, leaving only the one chaotic attractor.

3.3.2. *From limit cycle, pitchfork and homoclinic bifurcation to chaos*

Consider now the dynamics when c decreases from $+\infty$. The equilibrium at the origin has one eigenvalue of -2.6667, and the other two eigenvalues satisfy Eq. (5). According to the Hopf bifurcation theorem [Casti, 2000], there is a Hopf bifurcation at $c = 10$. The origin is globally stable for $c \in (8, 10)$. At $c = 8$, the origin loses stability by a supercritical pitchfork bifurcation and a symmetric pair of attracting fixed points are born. At $c = 7.7567$, the eigenvalues, which are a complex conjugate pair, cross the imaginary axis at a supercritical Hopf bifurcation where a pair of coexisting stable limit cycles are born. The dimension of the attractors changes from zero (a point) to one (a closed loop), and the first Lyapunov exponent is zero and the second Lyapunov exponent is negative.

For c decreasing from this point, the two coexisting unstable limit cycles expand as shown in Figs. 7(a) and 7(b) and then merge at $c = 7.6792$ as shown in Fig. 7(c). The merged limit cycle grows with decreasing c as shown in Fig. 7(d). When c decreases further, a pitchfork bifurcation appears at $c = 7.075$ where the attractor splits into two as shown in Fig. 7(e). Then one circle of the attractor grows while the other circle shrinks with decreasing c as shown in Fig. 7(f). At $c = 7.054$, the cycles touch the saddle point and become homoclinic orbits, and hence we have a homoclinic bifurcation and the onset of chaos as shown in Fig. 7(g). At that point, the largest Lyapunov exponent switches

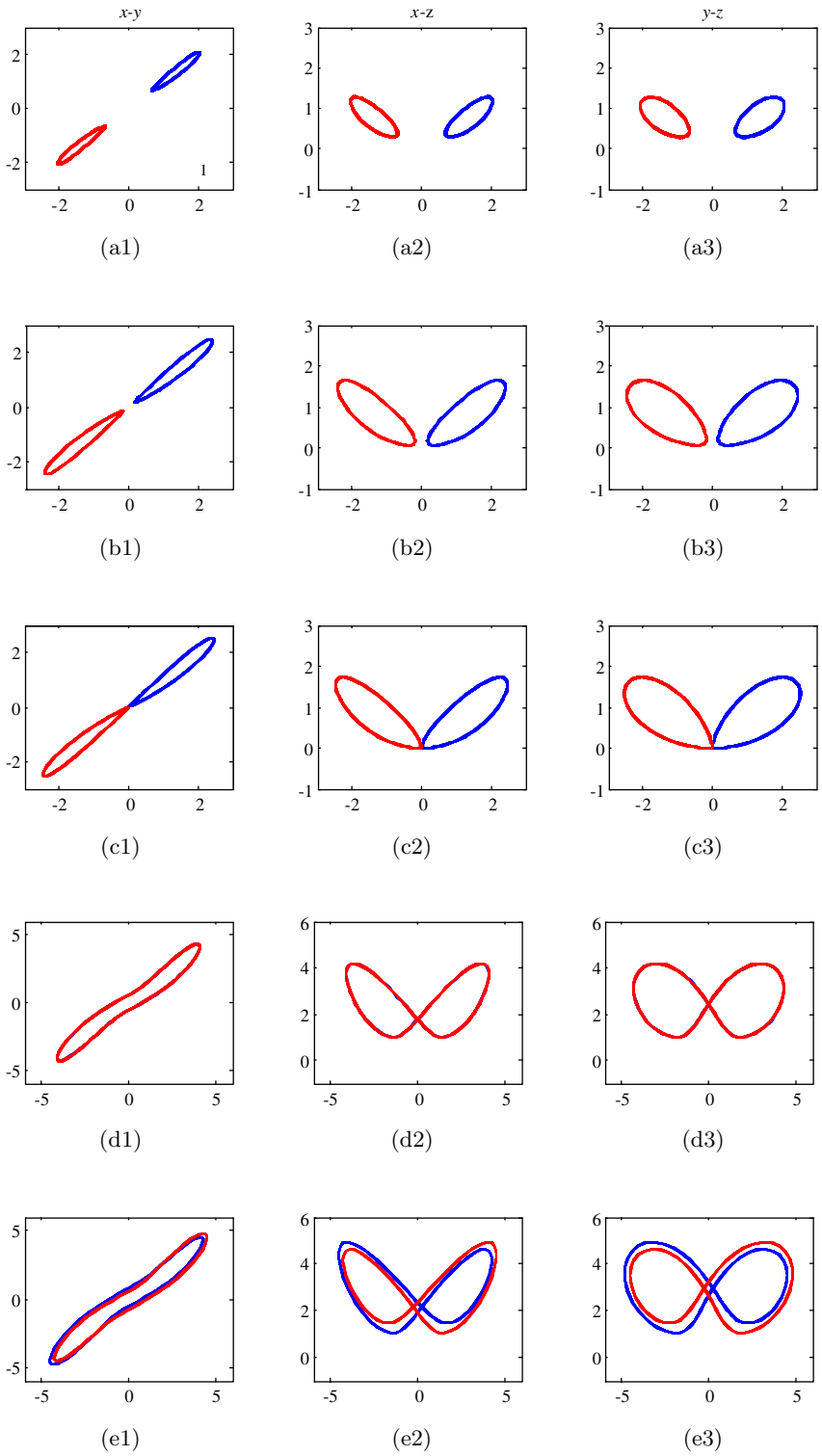

Fig. 7. State space plots for different c (blue and red attractors correspond to two symmetrical initial conditions): (a) $c = 7.73$, (b) $c = 7.69$, (c) $c = 7.6792$, (d) $c = 7.2$, (e) $c = 7.075$, (f) $c = 7.06$, (g) $c = 7.05$.

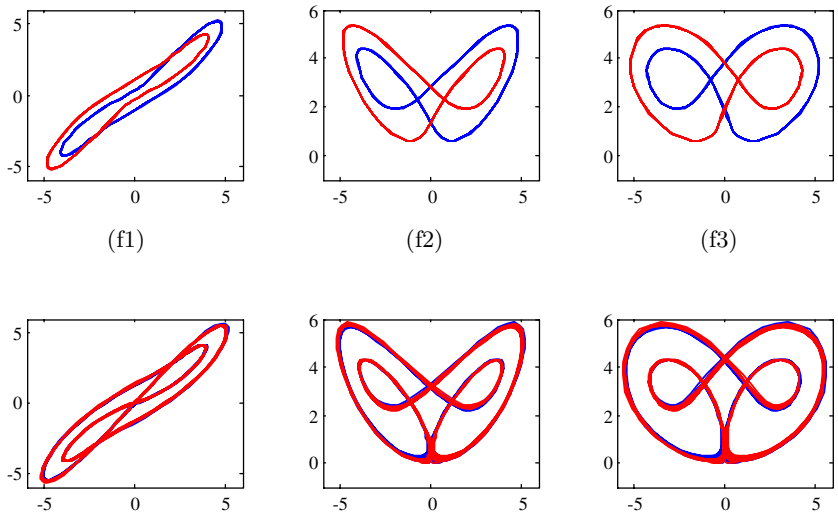

Fig. 7. (*Continued*)

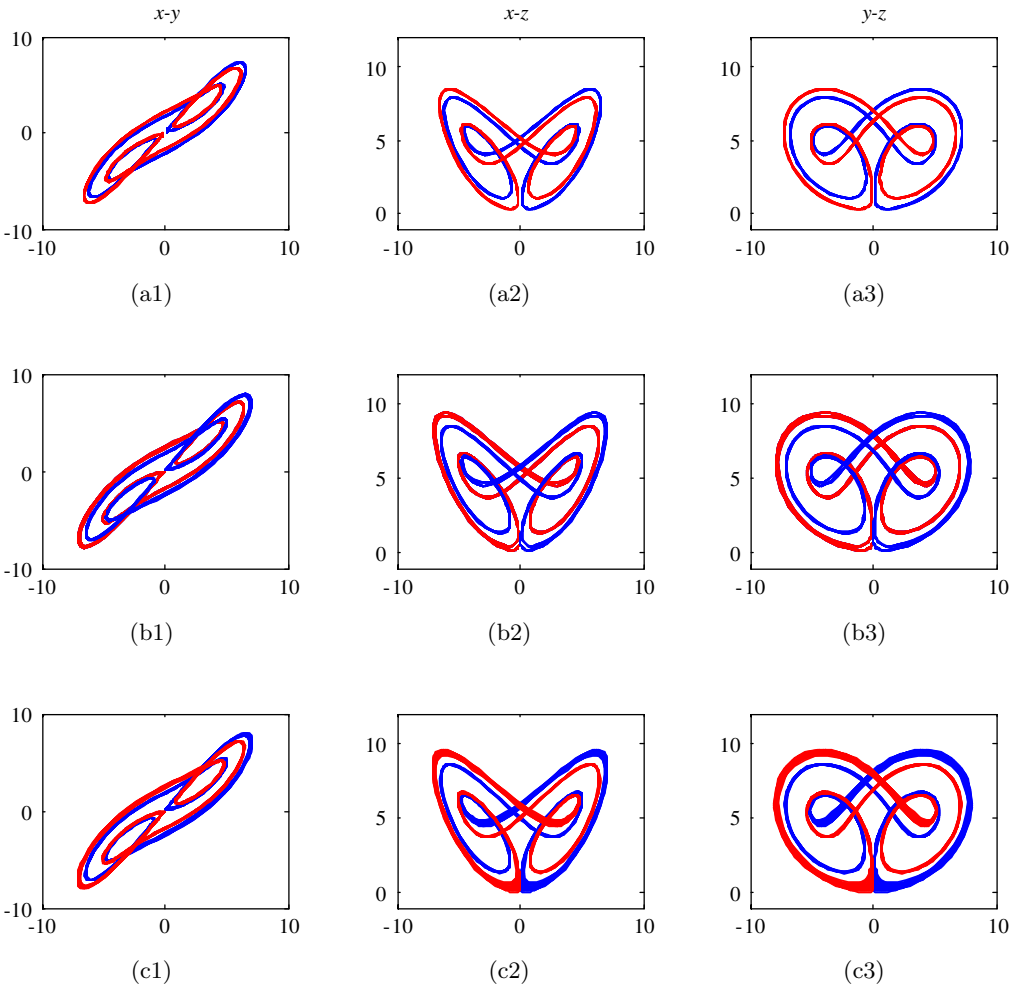

Fig. 8. State space plots for different c (blue and red attractors correspond to two symmetrical initial conditions): (a) $c = 6.60$, (b) $c = 6.46$, (c) $c = 6.442$, (d) $c = 6.44$.

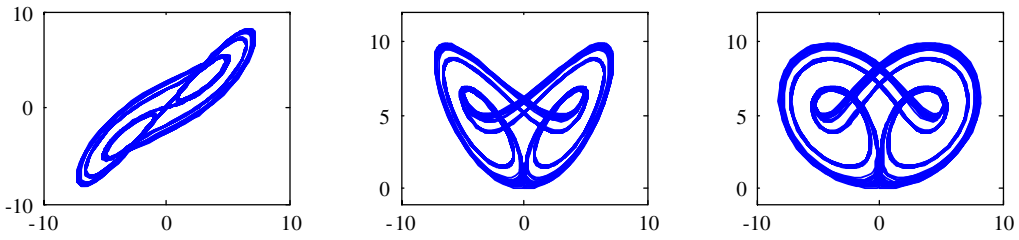

Fig. 8. (*Continued*)

from zero to positive, while the second Lyapunov exponent switches from negative to zero, and the dimension changes from one to a value slightly in excess of two.

3.3.3. *Behaviors in the periodic windows*

In certain ranges of c, there are periodic windows, including large ones at $c \in (6.44, 6.80)$ and $c \in (6.13, 6.35)$ where dynamics similar to that described above occur. For example, in the window at $c \in (6.44, 6.80)$, a pitchfork bifurcation occurs at $c = 6.60$ where two coexisting stable limit cycles are born as shown in Fig. 8(a). For $c \in (6.80, 6.47)$, there are two periodic attractors, each of which is composed of two single circles separated at the bottom. As c decreases, the periodic orbit changes through a period-doubling bifurcation at $c = 6.46$ as shown in Fig. 8(b). At $c = 6.442$, the outside circle doubles again as shown in Fig. 8(c). Finally, it gives way to chaos by homoclinic bifurcation at $c = 6.44$, and the coexisting state disappears as shown in Fig. 8(d). Hence the route to chaos in this window is complex, including a pitchfork bifurcation, period-doubling bifurcations and a homoclinic bifurcation.

4. Conclusion

This paper has reported and analyzed a variant of the Lorenz system in which one parameter is varied. Two values of that parameter ($c = 0$ and $c = 6$) correspond, respectively, to simplifications of the Lorenz system in which one or the other of the linear terms in the $\dot{y}$ equation is set to zero, and a third value ($c = -1$) corresponds to the standard Lorenz system. The dynamical properties of this chaotic system have been analyzed, including the Lyapunov exponents, fractal dimension and routes to chaos. The results show it displays abundant and complex dynamics. There are additional interesting features of this system in terms of control, synchronization, circuit implementation and its application to secure communications that deserve further study.

Acknowledgments

This work was supported by the China Scholarship Council (No. 2006A39010), the National Nature Science Foundation of People's Republic of China (Grant No. 60672041), and the National Science Foundation for Post-doctoral Scientists of People's Republic of China (Grant No. 20070420774). We are grateful for discussions with Prof. George Rowlands.

References

Casti, J. L. [2000] *Five More Golden Rules: Knots, Codes, Chaos, and Other Great Theories of 20th-Century Mathematics* (Wiley, NY), pp. 55–99.

Chen, G. & Ueta, T. [1999] "Yet another chaotic attractor," *Int. J. Bifurcation and Chaos* **9**, 1465–1466.

Elwakil, A. S. & Kennedy, M. P. [2001] "Construction of classes of circuit_independent chaotic oscillators using passive-only nonlinear devices," *IEEE Trans. Circuits Syst. I* **48**, 289.

Kaplan, J. & Yorke, J. [1979] "Chaotic behavior of multidimensional difference equations," in *Functional Differential Equations and Approximations of Fixed Points*, Lecture Notes in Mathematics, Vol. 730, eds. Peitgen, H.-O. & Walther, H.-O. (Springer, Berlin), pp. 228–237.

Lorenz, E. N. [1963] "Deterministic nonperiodic flows," *J. Atmos. Sci.* **20**, 130–141.

Lü, J. & Chen, G. [2002] "A new chaotic attractor coined," *Int. J. Bifurcation and Chaos* **12**, 659–661.

Lü, J., Chen, G., Cheng, D. & Celikovsky, S. [2002] "Bridge the gap between the Lorenz system and the Chen system," *Int. J. Bifurcation and Chaos* **12**, 2917–2926.

Lü, J., Chen, G. & Zhang, S. [2004] "Dynamical analysis of a new chaotic attractor," *Int. J. Bifurcation and Chaos* **12**, 1001–1015.

Qi, G., Chen, G. & Du, S. [2005] "Analysis of a new chaotic system," *Physica A* **352**, 295–308.

Rössler, O. E. [1976] "An equation for continuous chaos," *Phys. Lett. A* **57**, 397–398.

Stewart, I. [2000] "The Lorenz attractor exists," *Nature* **406**, 948–949.

Ueta, T. & Chen, G. [2000] "Bifurcation analysis of Chen's attractor," *Int. J. Bifurcation and Chaos* **10**, 1917–1931.

Vaněček, A. & Čelikovský, S. [1996] *Control Systems: From Linear Analysis to Synthesis of Chaos* (Prentice-Hall, London).

Wolf, A., Swift, J., Swinney, H. & Vastano, J. [1985] "Determining Lyapunov exponents from a time series," *Physica D* **16**, 285–317.

Yorke, J. A. & Yorke, E. D. [1979] "Metastable chaos: The transition to sustained chaotic behavior in the Lorenz model," *J. Stat. Phys.* **21**, 263–276.

Zhu, L., Raghu, A. & Lai, Y.-C. [2001] "Experimental observation of superpersistent chaotic transients," *Phys. Rev. Lett.* **86**, 4017–4020.

Copyright of International Journal of Bifurcation & Chaos in Applied Sciences & Engineering is the property of World Scientific Publishing Company and its content may not be copied or emailed to multiple sites or posted to a listserv without the copyright holder's express written permission. However, users may print, download, or email articles for individual use.